

Synchrotron x-ray studies of vitreous SiO<sub>2</sub> over Si(001). II. Crystalline contributionM. Castro-Colin,<sup>1</sup> W. Donner,<sup>1</sup> S. C. Moss,<sup>1,2</sup> Z. Islam,<sup>3</sup> S. K. Sinha,<sup>4</sup> and R. Nemanich<sup>5</sup><sup>1</sup>Physics Department., University of Houston, Houston, Texas 77204-5005, USA<sup>2</sup>Texas Center for Superconductivity and Advanced Materials, University of Houston, Houston, Texas 77204, USA<sup>3</sup>Advanced Photon Source, Argonne National Laboratory, Argonne, Illinois 60439, USA<sup>4</sup>Department of Physics, University of California San Diego, California 92093-0354, USA<sup>5</sup>Department of Physics, North Carolina State University, Raleigh, North Carolina 27695, USA

(Received 9 July 2004; published 13 January 2005)

Thermally oxidized thin films grown on Si(001) were analyzed with synchrotron x rays. By looking at crystal truncation rod (CTR) profiles we were able to observe, as have others, a crystalline peak, nominally along the  $(1\ 1\ L)$  rod, together with Laue oscillations matching the film thickness. These oscillations are evidence of a crystalline component present throughout the entire film that vanishes away from the interface with the silicon substrate. A model consisting of distorted coesite is proposed to explain the results.

DOI: 10.1103/PhysRevB.71.045311

PACS number(s): 68.47.Gh, 61.10.Eq, 61.43.Fs, 78.70.Ck

## I. INTRODUCTION

As noted in paper I,<sup>32</sup> the technical importance in the semiconductor industry of thermally grown amorphous SiO<sub>2</sub> on crystalline Si(001), has resulted in intense interest<sup>1-12</sup> over the years. We have, on the one hand, the obvious practical applications that may entail thinner and more reliable integrated circuits, but there are also more basic features underlying this system. An amorphous material, SiO<sub>2</sub>, is in close contact with a crystalline, Si(001), substrate, and the properties of SiO<sub>2</sub> are such that an incipient crystalline component makes itself evident within the amorphous matrix. Rochet *et al.*<sup>4</sup> observed by high-resolution transmission electron microscopy (HRTEM), crystallites growing in registry with the Si $\langle 110 \rangle$  and Si $\langle \bar{1}\bar{1}0 \rangle$  throughout the film; a condition included in our model. Iida *et al.*<sup>1</sup> used (as in the present work) x-ray crystal truncation rod (CTR) scattering to probe the film, and observed a peak along the Si $\langle 111 \rangle$  rod at  $(1\ 1\ 0.45)$ . This peak vanished after etching away the oxidized layer, as a clear indication of its origination in the film. Harada and co-workers<sup>2</sup> carried out a thorough CTR analysis, and proposed a model based on distorted cristobalite distributed within the entire film, to explain the crystalline peak along the Si $\langle 1\ 1\ L \rangle$  ( $L$  is a continuous reciprocal lattice unit, r.l.u.) rod. They<sup>2</sup> had the appropriate resolution to register Laue oscillations along this rod, whose period represented the film thickness. To our knowledge, the most recent experiments using the CTR technique on this system were performed by Munkholm *et al.*<sup>3</sup> and Tatsumura *et al.*<sup>12</sup> Both results<sup>3,12</sup> showed oscillations and the crystalline peak. One group<sup>3</sup> attributed the observations to columnar grains of an ordered oxide without proposing a particular crystalline phase and with no analysis of the intensity. The other group<sup>12</sup> used numerical simulations with molecular dynamics (to oxidize crystalline silicon), to subsequently calculate the x-ray scattering along the Si $\langle 1\ 1\ L \rangle$  rod. From the findings they<sup>12</sup> suggested that residual order, from a highly distorted cristobalite-like structure, generates the crystalline peak observed.

The present work seeks to complement our results already presented<sup>32</sup> in paper I [concerning a fourfold modulation of

the first sharp diffraction peak (FSDP) of thin SiO<sub>2</sub> along Si $\langle 110 \rangle$  and Si $\langle \bar{1}\bar{1}0 \rangle$ , and a compressed interfacial region], and also to offer a different<sup>1-3,5,12</sup> and plausible model via a coesite-like crystalline phase. The crystalline component discussed here is seen as additional evidence of the loss of isotropy in the amorphous SiO<sub>2</sub> when in contact with a highly symmetric substrate, Si(001).

## II. MATERIALS AND METHODS

As previously noted in paper I,<sup>32</sup> the thin film samples under investigation were prepared, at North Carolina State University, with an RCA cleaning that leaves a thin native oxide on  $p$ -type Si(001) oriented. The samples showed a miscut of  $\approx 0.2^\circ$  at  $\approx 5^\circ$  off the  $\langle 100 \rangle$ . Two samples were grown at 1123 K for 30 min and 1223 K for 66 min to produce 100 and 500 Å SiO<sub>2</sub> films (reported from ellipsometry), respectively.

At the Advanced Photon Source (APS), beamline 4-ID-D, the experiment was done at 20 keV ( $\lambda = 0.6199$  Å). A sample of 100 Å SiO<sub>2</sub>/Si was placed inside a beryllium can filled with helium gas to reduce the background contribution. With the wavelength available, the critical angle for total external reflection was  $\alpha_c = 0.087^\circ$ . Using grazing-incidence diffraction (GID) geometry, and a scintillation detector, the  $(\frac{5}{2}\ 0\ L)$ ,  $(\frac{3}{2}\ 0\ L)$ , and  $(\frac{1}{2}\ 0\ L)$  rods ( $L = 0.5 \rightarrow 8.0$ ) were investigated, as well as other half-order reflections like  $(\frac{1}{2}\frac{1}{2}\ 0)$  and  $(\frac{1}{2}\ 1\ 0)$ , to search for evidence of a  $(2 \times 1)$  surface reconstruction<sup>13-15</sup> that might have existed at the interface between Si(001) and the oxidized layer. In particular, Renaud *et al.*,<sup>14</sup> as well as Yu and Tersoff in a Monte Carlo theoretical study,<sup>16</sup> favored the existence of an ordered interfacial structure related to a  $(2 \times 1)$  reconstruction. However, we could find no evidence of half-order reflections, along the aforementioned rods, as earlier discussed in a work<sup>13</sup> about the surface of dry thermally oxidized Si(001).

To investigate the  $(1\ 1\ L)$  CTR, the geometry shown in the upper inset of Fig. 1 was used at the APS.  $L$  varied between

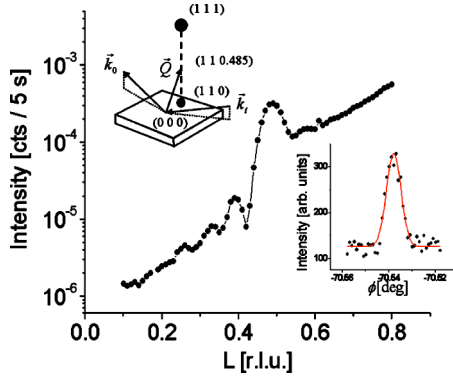


FIG. 1. (Color online) Si(1 1  $L$ ) rod. Upper inset: scanning geometry. Lower inset:  $\phi$ -scan profile characteristic of every scan across the  $L$  positions.

0.1 and 0.8 r.l.u. A series of  $\phi$  scans (lower inset) collected the intensity, at every  $L$  position, to construct the truncation rod profile (over background) in Fig. 1. From the full width at half maximum (FWHM) of the  $\phi$  scan ( $0.007^\circ$ ), shown in the inset, we estimate a coherent domain size  $L_c \approx 9800 \text{ \AA}$ , which is quite large due to a combination of the (1 1 0) Si rod and the crystalline  $\text{SiO}_2$  rod.

The sample of  $500 \text{ \AA}$   $\text{SiO}_2$  was analyzed, with  $10 \text{ keV}$  ( $\lambda = 1.239 \text{ \AA}$ ), at the APS. To study the behavior of the (1 1  $L$ ) truncation rod in the  $500 \text{ \AA}$  film, we used a NaI scintillation detector. A set of data points gave information in a  $1 KL$  region (Fig. 2) in reciprocal space;  $H = 1 \text{ r.l.u.}$ ,  $K = 0.99398 \rightarrow 1.0045 \text{ r.l.u.}$ ,  $L = 0.3 \rightarrow 0.6 \text{ r.l.u.}$ . The cross sections in Fig. 2 exhibit a FWHM of  $0.00041 \text{ r.l.u.}$  (*sharp* feature, resolution limited) and  $0.00361 \text{ r.l.u.}$  (*broad* feature); the integrated intensity of both features varies in a similar fashion along  $\langle 1 1 L \rangle$ . From the FWHM of the broad feature, a coherent domain size  $L_c = a_{\text{Si}}/w \approx 1500 \text{ \AA}$  ( $w$  is the width, in r.l.u.) can be extracted. For the sharp feature  $L_c$  is approximately ten times larger. Note that the broad and sharp features were not discriminated in the  $100 \text{ \AA}$  measurement at  $\lambda = 0.6199 \text{ \AA}$  due to lower resolution. This, therefore, does not permit a clear comparison of the coherent domain size between  $100$  and  $500 \text{ \AA}$  films. We would note that the study of Munkholm *et al.*<sup>3</sup> showed much smaller coherent domain sizes for their proposed columns.

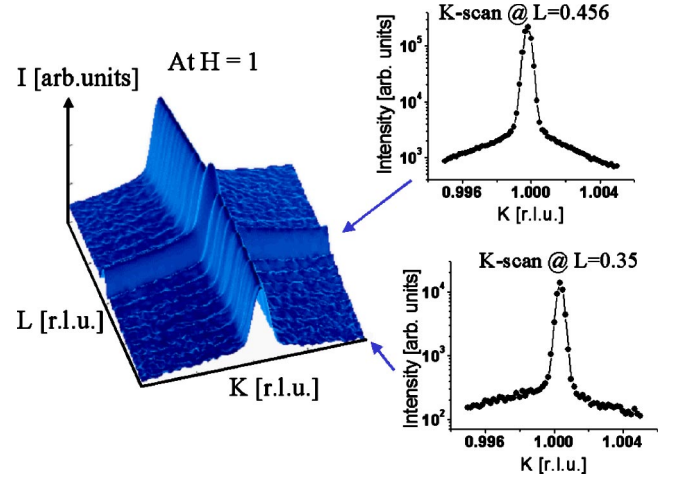


FIG. 2. (Color online)  $1KL$  map of  $500 \text{ \AA}$  film. The insets show cross sections at  $L = 0.35$  and  $L = 0.456 \text{ r.l.u.}$ , where broad and sharp features can be observed.

### III. RESULTS AND DISCUSSION

The model proposed in this study, as the constituent of the  $\text{SiO}_2/\text{Si}(001)$  interface, differs from those presented by others.<sup>2,5,10,16–20</sup> The approach followed here, to tailor the model, has been that of fitting the measured Si CTR's, bearing in mind the FSDP intensity enhancement (discussed in detail earlier in paper I) observed in the GID measurements of both samples,  $100 \text{ \AA}$  and  $500 \text{ \AA}$   $\text{SiO}_2$  films. As will be pointed out later, the  $\text{SiO}_2$  crystalline peak arises when the scattering of both substrate and crystalline components add their amplitudes in a coherent fashion. This  $\text{SiO}_2$  crystalline peak, has, to date, only been observed<sup>1–3,12</sup> along the (1 1  $L$ ) rod of Si.

The peak observed along the Si(1 1  $L$ ) rod has a maximum at  $L_{\text{max}} = 0.485$  and  $0.455 \text{ r.l.u.}$ , for  $100 \text{ \AA}$  and  $500 \text{ \AA}$  films, respectively. This value indicates a lattice spacing in the direction normal to the surface  $c_{c\text{-SiO}_2} = a_{\text{Si}}/L_{\text{max}} \approx 11.198$  and  $\approx 11.936 \text{ \AA}$  for  $100$  and  $500 \text{ \AA}$  films (the index  $c\text{-SiO}_2$  indicates a crystalline  $\text{SiO}_2$  phase, as distinguished from an amorphous one  $a\text{-SiO}_2$ ), respectively.

In Table I, a list of densities and lattice parameters of several  $\text{SiO}_2$  polymorphs is presented. Coesite has been chosen as the precursor of a plausible initial model (pseudocoes-

TABLE I. Some  $\text{SiO}_2$  polymorphs, including their densities and lattice parameters, from Ref. 22.

Polymorph	$\rho(\text{g/cm}^3)$	$a(\text{\AA})$	$b(\text{\AA})$	$c(\text{\AA})$	$\alpha$	$\beta$	$\gamma$
Glass	2.1900	-	-	-	-	-	-
$\alpha$ -quartz	2.6458	4.9160	4.9160	5.4050	$90^\circ$	$90^\circ$	$120^\circ$
$\alpha$ -cristobalite	2.3572	4.9570	4.9570	6.8903	$90^\circ$	$90^\circ$	$90^\circ$
$\beta$ -cristobalite	2.1746	7.1600	7.1600	7.1600	$90^\circ$	$90^\circ$	$90^\circ$
Stishovite	4.2808	4.1801	4.1801	2.6150	$90^\circ$	$90^\circ$	$90^\circ$
$\beta$ -tridymite	2.1833	8.7400	5.0500	8.2400	$90^\circ$	$90^\circ$	$90^\circ$
Keatite	2.4987	7.4560	7.4560	8.6040	$90^\circ$	$90^\circ$	$90^\circ$
Coesite	2.9215	7.1600	12.3900	7.1600	$90^\circ$	$\neq 90^\circ$	$90^\circ$

ite, PC), because it involves the smallest average percentage variation of its unit cell parameters. Variations in the in-plane (parallel to the film surface) parameters average 7.2% ( $a$  and  $c$  in Table I), by comparison to the distance along Si(110) (7.680 Å) in a Si unit cell. The unit cell variation normal to the film surface averages 6.6% ( $b$  in Table I). The unit cell parameters (500 Å film) chosen for the PC model are  $a = 7.60$  Å,  $c = 7.62$  Å,  $b = 11.93$  Å,  $\alpha = \gamma = 90^\circ$ , and  $\beta = 119.6^\circ$ . With the lattice parameters chosen for PC, the density is now  $\approx 2.31$  g/cm<sup>3</sup>; a lower density, if compared to that of actual coesite. The atomic coordinates of our “proposed” PC are given in Table II, used also to construct the PC unit cell.

PC and Si are considered to have a slightly mismatched epitaxial relationship as shown in Figs. 3 and 4, where the  $A_3$  PC closely matches the  $\langle 110 \rangle$  Si distance. This we believe, accounts in turn, for the peaking of the FSDP along  $[1\ 1\ 0]$  directions (paper I).<sup>32</sup>

To obtain the relationship between the Miller indices of PC and Si we use Fig. 3. From there we can calculate the unit cell vectors of PC,  $\vec{A}_i$ , in terms of those of Si,  $\vec{a}_i$ . By using the orthogonality properties ( $\vec{A}_i \cdot \vec{A}_j^* = 2\pi\delta_{ij} = \vec{a}_i \cdot \vec{a}_j^*$ ) of the unit cell vectors and the reciprocal lattice vectors ( $\vec{A}_i^*, \vec{a}_i^*$ ), in the corresponding PC and Si systems, we obtain the set of equations

$$\begin{aligned} -1.34913H + 0.37161K &= h, \\ 2.19666L &= k, \\ 0.99211H + 0.99211K &= l, \end{aligned} \quad (1)$$

where  $h, k, l$  are the PC Miller indices and  $H, K, L$  are those of Si. With the aid of the coordinate transformations in Eq. (1), and the expression of the structure factor ( $F_{HKL} = \sum_n f_{\text{Si}(n), \text{O}(n)} e^{i2\pi(Hx_n + Ky_n + Lz_n)}$ ;  $f_{\text{Si}(n), \text{O}(n)}$  are the atomic form factors of Si and O, respectively), some PC reflections can be related to the Si reciprocal space system (500 Å film):

$$\begin{aligned} F_{(110.455)}^{\text{Si}} : 59.05 &= F_{(\bar{1}12)}^{c\text{-SiO}_2}, \\ F_{(220)}^{\text{Si}} : 325.68 &= F_{(204)}^{c\text{-SiO}_2}, \\ F_{(110)}^{\text{Si}} : 0 &= F_{(102)}^{c\text{-SiO}_2}, \\ F_{(111.365)}^{\text{Si}} : 100 &= F_{(132)}^{c\text{-SiO}_2}, \end{aligned} \quad (2)$$

The notation chosen stresses the fact that the structure factor corresponds to the crystalline phase, but it also has a coincidence in reciprocal space with Si. The reflection that coincides with Si(11  $a_{\text{Si}}/b$ ) (shown later in Figs. 6 and 7) corresponds to that of the crystalline peak along the CTR. Si(2 2 0) is allowed in Si as is its equivalent reflection in PC. On the other hand, Si(1 1 0) is forbidden in Si as is its equivalent reflection in PC. Taking as an example the calculations for the 500 Å film, there is one reflection that is allowed in PC and would have a coincidence with Si(1 1 1.365), but it is not observed in any of the actual measure-

TABLE II. Atomic coordinates of coesite (Ref. 22).

Atom	Wyck.	$x$	$y$	$z$
Si(1)	8 <i>f</i>	0.140	0.108	0.074
Si(2)	8 <i>f</i>	0.506	0.158	0.539
O(1)	4 <i>a</i>	0.000	0.000	0.000
O(2)	4 <i>e</i>	0.500	0.117	0.750
O(3)	8 <i>f</i>	0.269	0.126	0.941
O(4)	8 <i>f</i>	0.308	0.103	0.329
O(5)	8 <i>f</i>	0.012	0.212	0.473

ments along the Si(1 1  $L$ ) rod.<sup>2,21</sup> This last issue needs more careful study,<sup>12</sup> especially in consideration of the extensive strain suffered by the proposed PC, which should have a considerably larger transverse component (normal to  $L$ ) at Si(0 0 0.455) than at Si(0 0 1.365). This means that there will be a significantly greater attenuation at (0 0 1.365) than at (0 0 0.455) because the structure factor contains, in principle, a term  $\propto (\vec{Q} \cdot \vec{\delta})^2$  where  $\vec{\delta}$  is the transverse component of the displacement parallel to the Si sample.

We note here that we use PC for a specific reason: although the crystalline component is reasonably well matched it is certainly not a perfect coesite crystal, and is furthermore a high pressure phase of SiO<sub>2</sub>. Here the demands of coherent epitaxy provide the necessary strain. It must then, as noted above, be quite disordered as it needs to be coherently connected to the vitreous SiO<sub>2</sub>, and this implies both distortion of the coesite (here PC) and an orientation and strain of the glass film. It is part of our ongoing work to find, via a Monte Carlo relaxation, a picture of a single coesite crystal within the amorphous film. Tatsumura *et al.*<sup>12</sup>, in a very interesting work, numerically simulated the x-ray scattering from a structure obtained through oxidation of crystalline silicon. They<sup>12</sup> suggested that it is only a residual order, arising from the {1 1 1} planes in their parent crystals, remaining after the oxidation process, which is responsible for the single  $c$ -SiO<sub>2</sub> reflection observed along the Si(1 1  $L$ ) rod. Large amounts of static disorder in a weakly crystalline cristobalitelike structure, would suppress any further higher-order reflections.

In our case, the Si truncation rods are modeled out of the next equation, using the following, in which, because of the

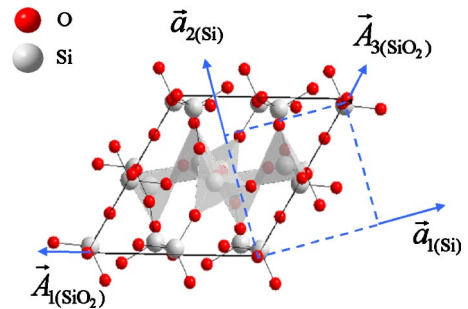


FIG. 3. (Color online) Proposed epitaxial relationship of the pseudocoesite unit cell respect to the Si unit cell; view normal to the film surface.

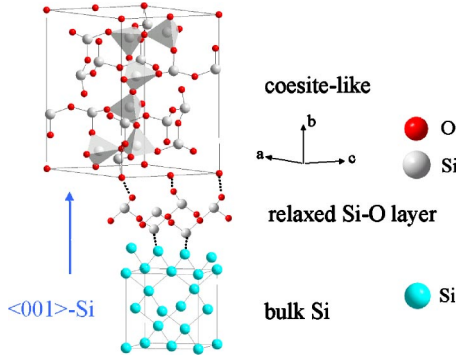


FIG. 4. (Color online) Epitaxial relationship of the pseudocoosite unit cell respect to the Si unit cell.

coherence of the crystallite rods and the Si(001), amplitudes are added rather than intensities:

$$\begin{aligned}
 F_{HKL} = & W_{\text{Si}} \frac{e^{-(2\pi[L-1]\sigma_{\text{Si}})^2}}{1 - e^{-i2\pi L}} F_{HKL}^{\text{Si}} + W_{\text{O,Si}} f_{\text{O,Si}} e^{-i2\pi L z_{\text{O,Si}}} \\
 & + W_{c\text{-SiO}_2} F_{HKL}^{c\text{-SiO}_2} e^{-(2\pi[L-b/a_{\text{Si}}]\sigma_{c\text{-SiO}_2})^2} e^{i2\pi L \Delta} \\
 & \times \sum_{n=1}^{N_{c\text{-SiO}_2}} e^{-p(n-1)} e^{i2\pi n L b/a_{\text{Si}}}. \quad (3)
 \end{aligned}$$

The first term in Eq. (3) accounts for the Si truncation rod, whose components are the typical exponential decay, a roughness factor  $e^{-(2\pi[L-1]\sigma_{\text{Si}})^2}$ , and a weight factor  $W_{\text{Si}}$  that aids in scaling the interfacial ( $W_{\text{O,Si}}$ ) and the  $c$ - $\text{SiO}_2$  ( $W_{c\text{-SiO}_2}$ ) contributions. These weighting factors are simply a representation of the surface coverage of each phase.  $L-1$  appears because we are measuring down from the Si(1 1 1). The second term represents the interfacial structure, formed by Si and O atoms ( $f_{\text{Si,O}}$ ), displaced solely normal to the sample surface. This is essentially the only information (displacements normal to the film) that we can currently extract from the CTR measurements, because of the limited amount of information provided by a single rod. The last term contains the crystalline phase influence, formed by the PC structure factor, with the lattice mismatched and phase-shifted in the  $L$  direction, by an amount  $\Delta$ , a roughness

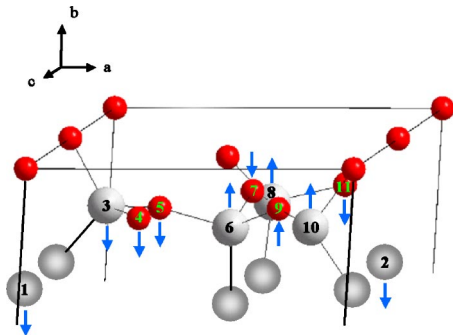


FIG. 5. (Color online) Proposed interfacial atoms (from fitting process), labeled with numbers (Table III) and their displacements (500 Å film).

TABLE III. Coordinates and displacements of interfacial atoms. Two oxygen atoms in the original PC unit cell were substituted by Si atoms, highlighted as  $^*\text{Si}$ .

Atom	$x$	$y$	$z$ (500 Å film)	$z$ (100 Å film)
$^*\text{Si}(1)$	0.012	0.788	$0.973-0.010$	$0.973+0.055$
$^*\text{Si}(2)$	0.988	0.788	$0.527-0.025$	$0.527+0.026$
Si(3)	0.140	0.892	$0.574-0.010$	$0.574-0.034$
O(4)	0.308	0.897	$0.829-0.031$	$0.829+0.146$
O(5)	0.269	0.874	$0.441-0.040$	$0.441-0.025$
Si(6)	0.494	0.842	$0.461+0.007$	$0.461+0.017$
O(7)	0.500	0.883	$0.250-0.041$	$0.250+0.119$
Si(8)	0.506	0.842	$0.039+0.023$	$0.039+0.027$
O(9)	0.692	0.897	$0.671+0.091$	$0.671-0.074$
Si(10)	0.860	0.892	$0.926+0.172$	$0.926-0.115$
O(11)	0.731	0.874	$0.059-0.059$	$0.059-0.089$

factor  $e^{-(2\pi[L-b/a_{\text{Si}}]\sigma_{c\text{-SiO}_2})^2}$ , and a summation [the factor of  $b/a_{\text{Si}}$  represents the ratio of PC ( $b=c_{c\text{-SiO}_2}$  unit cell parameter) to the lattice parameter of Si ( $a_{\text{Si}}$ ) in order to place everything on a Si notation basis]. Such a summation takes into account the layers of crystallites that build up a portion of the film ( $N_{c\text{-SiO}_2}$ ), as in Fig. 7 of paper I, and an occupation probability ( $e^{-p(n-1)}$ ) for each layer, to account for the decay of the crystalline fraction from the interface to the surface, much the same as with the decay of the modulated glass (as discussed in paper I). The formalism used here closely follows that of an earlier study of Harada and co-workers.<sup>2</sup> A least-squares minimization helped with the fitting method.

The atomic displacements at the interface are pictured in Fig. 5. 11 atoms from a PC unit cell, the uppermost, are used to construct the interface. They are labeled for easier identification, and the arrows indicate the direction of the displacements, as obtained from the fitting procedure. Two oxygen atoms in the original PC unit cell were substituted by Si atoms, these last highlighted as  $^*\text{Si}$  in Table III, where all coordinates and displacements are summarized. Other fitting parameters are given in Table IV. The curves obtained using the fitting parameters proposed are found in Figs. 6 and 7.

In Fig. 7(a), inset, we display a curve obtained when the displacements in Table III are not included. Such displacements

TABLE IV. Fitting parameters.

Atom	500 Å film	100 Å film
$W_{\text{Si}}$	23.500	18.500
$\sigma_{\text{Si}}$	1.090	1.190
$W_{\text{Si,O}}$	15.000	14.800
$\Delta$	2.380	2.250
$W_{\text{SiO}_2}$	1.000	1.000
$\sigma_{\text{SiO}_2}$	1.630	1.456
$p$	0.034	0.172
$N_{c\text{-SiO}_2}$	36	7

ments contribute to the oscillatory line upon which the Laue oscillations appear. The Fig. 7(b) inset shows the crystalline occupation probability as a function of the layer number; the layer labeled as 1 denotes the interface.

A numerical fit of our results yielded an enhanced electron density 3% higher than that of the remaining SiO<sub>2</sub> film, as indicated by fitting the 100 Å reflectivity curve. Assuming a silica glass density<sup>22</sup> of 2.2 g/cm<sup>3</sup>, the enhanced density phase would have a value of 2.26 g/cm<sup>3</sup>; interestingly enough, this is a value close to the one estimated from the proposed model, ≈2.31 g/cm<sup>3</sup>, based on a coesitelike structure. Comparing such a value with those of other polymorphs, Table I, α-cristobalite, β-cristobalite, and tridymite, seem feasible crystalline phases (if we allow some distortion in the unit cell). We note that the unit cell parameters of coesite were modified less than 10% without appreciably (<2%) varying the dimensions of the structural units, the SiO<sub>4</sub> tetrahedra. Cristobalite, for instance, a precursor model chosen earlier,<sup>2,12,17,23</sup> requires distortions larger than 7% in the structural unit bond length. Tridymite has also been a likely candidate,<sup>5,19</sup> but it produces a crystalline peak at Si(1 1 0), where none is found (with the *c* axis oriented along Si(1 1 0)); additionally the crystalline peak along the Si(1 1 *L*) cannot be explained. It also requires equally large distortions in the tetrahedral structural units. Maintaining a low distortion in the structural units and a degree of lattice match along the Si(110), led us to chose coesite as a likely precursor crystalline phase that, distorted in a qualitative fashion, may exist embedded in the amorphous matrix. Recently, another group<sup>24</sup> published results using severely distorted pure Si to fit the same rod.

Truncation rods provided evidence of the incipient ordering of the amorphous film. The interfacial layer can be understood, out of the modeling here presented, as rather disordered, in agreement with recent studies,<sup>11,12</sup> and contrary to previous work.<sup>5,16</sup> The modeling presented up to now is only sensitive to variations normal to the film surface, those shown in Table III. There is no particular trend in those variations, meaning that a scaling that preserves directionality, from the 100 to the 500 Å film interface, is absent. Only the initial structure is common, but once the fitting process takes place, its evolution yields a different outcome, and there is no reason for any particular distortion value or peak position. Modeling of the truncation rods suggests an extended crystalline phase close to the interface, with a higher proportionality of crystallites in the 100 Å than in the 500 Å film, which essentially vanish at the surface of the 500 Å film, much as the fourfold <110> oriented glass, with which it is intimately connected. The interface model proposed makes use of suboxidized silicon species,<sup>7,25–27</sup> with which the model here proposed also suggests a gradual ordering transition at the interface. This model currently only considers Si<sup>3+</sup> species, although Si 2*p* core level spectroscopy<sup>25–27</sup> and electron energy-loss spectroscopy<sup>7</sup> additionally measure Si<sup>1+</sup> and Si<sup>2+</sup> species at the interface.

Roughness values produced by the truncation rod fittings differ from that found in our reflectivity fit. But one must bear in mind that while in the rods there is an explicitly stated interface, in the reflectivity, the strata have an ex-

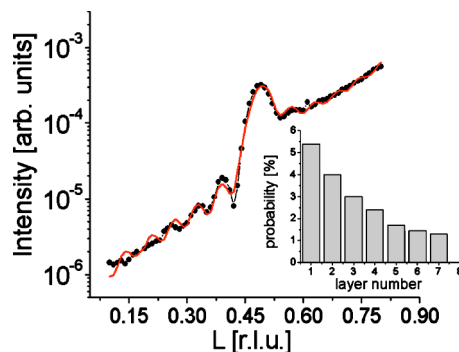


FIG. 6. (Color online) Fitted profile of 100 Å film; full circles denote experimental results, the red line is the fit. The inset shows the crystallite occupation probability as a function of the layer number, with the interface at the left, layer no. = 1.

tended average roughness value that associates an electron density gradient between strata. In the truncation rod fit, atomic displacements of the interfacial structure can be understood to account for the reduced roughness, which is actually “constructed” over a more localized region (the lateral extent of the crystallite), by comparison to that of the reflectivity. Roughness has the effect of reducing the intensity, and that is part of the effect imprinted by the atomic interfacial displacements. In any case an rms roughness value of 5 Å (as obtained in the reflectivity fit) is less than a unit cell of Si.

To be able to exhibit a more complete SiO<sub>2</sub> crystalline structure, a larger number of truncation rod and crystal reflection measurements are needed, and certainly, further modeling. At this point, their absence nonetheless does not invalidate the current model. Coesite is known to be a high-pressure SiO<sub>2</sub> phase, and that may be seen as a counterargument for the likelihood of its existence within a thin film. But it is also well known that the strain that accompanies the epitaxial growth of thin films<sup>28</sup> on substrates is often greater than the pressure needed to produce the phase in bulk; hence our choice of pseudocoesite. Additionally, the density associated with pseudocoesite is lower than that of actual coesite.

As it is widely accepted, SiO<sub>2</sub> is composed of four oxygen atoms (O) shaping a tetrahedron that surrounds a silicon (Si)

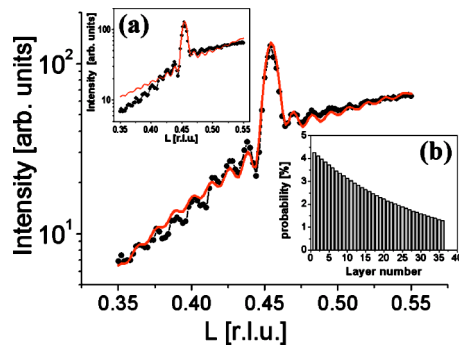


FIG. 7. (Color online) Fitted profile of 500 Å film; full circles denote experimental results, the red line is the fit. The insets show (a) the best fit profile when the interfacial Si and O atoms are not included, (b) the crystallite occupation probability as a function of the layer number; again the interface is at the left.

atom. A basic structural unit,  $\text{SiO}_4$ , interacting with others of its type gives rise to all of the known  $\text{SiO}_2$  polymorphs. In the particular case we address here, it could be expected that  $\text{SiO}_4$  tetrahedra accommodate relative to each other, to fit along the  $\text{Si}[1\ 1\ 0]$  directions, and the oxidation dynamics then allows a polymorph to form. Simultaneously this phenomenon of preferential short- and medium-range order drives the glass modulation, expressed through its FSDP signature.<sup>29</sup>

Another perspective would have a crystalline polymorph formed during the oxidation process that amorphizes further during oxidation, integrating itself within the amorphous phase and leaving behind only a small percentage of crystallites. There could be a density gradient of crystallites, increasing towards the interface with crystalline silicon. As an instance of coexisting  $\text{SiO}_2$  phases, we can mention two interesting examples that involve coesite. Wittels<sup>30</sup> noted that in experiments with neutron-irradiated quartz, coesite presents stable regions (nonvitreous) at irradiation doses that completely disordered quartz, which most likely means that the host lattice can better sustain one phase over the other. One other example was offered by Bourret *et al.*,<sup>31</sup> who studied oxygen segregation and precipitation in bulk silicon, and proposed that coesite can be stabilized within the silicon matrix, over a wide range of temperatures. It is true that a silicon matrix surrounding precipitates containing oxygen constitutes quite a different system from the one currently studied; nevertheless there is a relation. The argument here is that, because the strain within the bulk can be large enough to permit coesite (or a coesitelike phase) to arise due to oxygen incorporated in the silicon matrix, such strain can be obtained in our thin films.<sup>28</sup>

To summarize the results of both papers I and II, we briefly note that a  $\text{SiO}_2$  glass anisotropy has been observed

under GID where the FSDP showed a fourfold modulation, indicating a compression along the  $\text{Si}[1\ 1\ 0]$  directions. This modulation vanishes close to the 500 Å film surface, which might set a limiting range of interaction (regarding the symmetry imprinted by the substrate) between the substrate and the film. A crystalline peak together with its Laue oscillations matching the film thickness, was observed along the  $\text{Si}(1\ 1\ L)$  rod, out of which, a model (crystalline  $\text{SiO}_2$ , coesitelike) was constructed to explain the findings, bearing in mind the glass anisotropy along the  $\text{Si}[1\ 1\ 0]$  directions. Such a model was proposed using only one reflection from the crystalline  $\text{SiO}_2$ , where a coesite polymorph was deformed to reflect the crystalline peak position and registry with the substrate.

We point out that there remain issues currently being addressed by us. These include computer relaxing the  $\text{SiO}_2$  glass in which a crystalline coesitelike phase is embedded, as this may give insight into the glass modulation. A more intense and systematic search for other  $c\text{-SiO}_2$  reflections<sup>2,12</sup> is necessary, to confirm (or refute) our proposed model.

#### ACKNOWLEDGMENTS

We acknowledge the assistance of J. C. Lang (4-ID-D, APS). M.C.-C. would like to acknowledge J. H. Li (UH) for useful discussions. This work was supported by the Department of Energy (DOE) under Contract No. DE-FG03-01ER45880. Use of the APS was supported by the U.S. DOE, Office of Science, Office of Basic Energy Sciences, under Contract No. W-31-109-Eng-38. Research carried at the NSLS, BNL, was supported by the U.S. DOE, Division of Materials Sciences and Division of Chemical Sciences, under Contract No. DE-AC02-98CH10886.

- 
- <sup>1</sup>Y. Iida, T. Shimura, J. Harada, S. Samata, and Y. Matsushita, *Surf. Sci.* **258**, 235 (1991).
- <sup>2</sup>I. Takahashi, T. Shimura, and J. Harada, *J. Phys.: Condens. Matter* **5**, 6525 (1993).
- <sup>3</sup>A. Munkholm, S. Brennan, F. Comin, and L. Ortega, *Phys. Rev. Lett.* **75**, 4254 (1995).
- <sup>4</sup>F. Rochet, S. Rigo, M. Froment, C. D'Anterrosches, C. Maillot, H. Roulet, and G. Dafour, *Adv. Phys.* **35**, 237 (1986).
- <sup>5</sup>A. Ourmazd, D. W. Taylor, J. A. Rentschler, and J. Bevk, *Phys. Rev. Lett.* **59**, 213 (1987).
- <sup>6</sup>E. P. Gusev, H. C. Lu, T. Gustafsson, E. Garfunkel, *Phys. Rev. B* **52**, 1759 (1995).
- <sup>7</sup>D. A. Muller, T. Sorsch, S. Moccio, F. H. Baumann, E. Evans-Lutterodt, and G. Timp, *Nature (London)* **399**, 758 (1999).
- <sup>8</sup>K. Hirose, H. Nohira, T. Koike, K. Sakano, and T. Hattori, *Phys. Rev. B* **59**, 5617 (1999).
- <sup>9</sup>A. Demkov and O. F. Sankey, *Phys. Rev. Lett.* **83**, 2038 (1999).
- <sup>10</sup>Y. Tu and J. Tersoff, *Phys. Rev. Lett.* **89**, 086102 (2002).
- <sup>11</sup>A. Bongiorno, A. Pasquarello, M. S. Hybertsen, and L. C. Feldman, *Phys. Rev. Lett.* **90**, 186101 (2003).
- <sup>12</sup>K. Tatsumura, T. Watanabe, D. Yamasaki, T. Shimura, M. Umeno, and I. Ohdomari, *Phys. Rev. B* **69**, 085212 (2004).
- <sup>13</sup>I. Hirose, K. Akimoto, T. Tatsumi, J. Mizuki, and J. Matisui, *J. Cryst. Growth* **103**, 150 (1990).
- <sup>14</sup>G. Renaud, P. H. Fuoss, A. Ourmazd, J. Bevk, B. S. Freer, and P. O. Hahn, *Appl. Phys. Lett.* **58**, 1044 (1991).
- <sup>15</sup>R. Felici, I. K. Robinson, C. Ottaviani, P. Imperatori, P. Eng, and P. Perfetti, *Surf. Sci.* **375**, 55 (1997).
- <sup>16</sup>Y. Tu and J. Tersoff, *Phys. Rev. Lett.* **84**, 4393 (2000).
- <sup>17</sup>S. T. Pantelides and M. Long, in *The Physics of SiO<sub>2</sub> and Its Interfaces*, edited by S. T. Pantelides (Pergamon, New York, 1978), p. 339.
- <sup>18</sup>M. Hane, Y. Miyamoto, and A. Oshiyama, *Phys. Rev. B* **41**, 12637 (1990).
- <sup>19</sup>A. Pasquarello, M. S. Hybertsen, and R. Car, *Phys. Rev. Lett.* **74**, 1024 (1995).
- <sup>20</sup>H. Kageshima and K. Shiraishi, *Phys. Rev. Lett.* **81**, 5936 (1998).
- <sup>21</sup>I. K. Robinson, *Phys. Rev. B* **33**, 3830 (1986).
- <sup>22</sup>R. B. Sosman, *The Phases of Silica* (Rutgers University Press, New Brunswick, 1965).
- <sup>23</sup>N. Awaji, Y. Sugita, Y. Horii, and I. Takahashi, *Appl. Phys. Lett.* **74**, 2669 (1999).
- <sup>24</sup>A. Munkholm and S. Brennan, *Phys. Rev. Lett.* **93**, 036106 (2004).

- <sup>25</sup>F. J. Himpsel, F. R. McFeely, A. Taleb-Ibrahimi, J. A. Yarmoff, and G. Hollinger, *Phys. Rev. B* **38**, 6084 (1988).
- <sup>26</sup>J. H. Oh, H. W. Yeom, Y. Hagimoto, K. Ono, M. Oshima, N. Hirashita, M. Nywa, A. Toriumi, and A. Kakizaki, *Phys. Rev. B* **63**, 205310 (2001).
- <sup>27</sup>C. Westphal, *Appl. Phys. A: Mater. Sci. Process.* **76**, 721 (2003).
- <sup>28</sup>C. P. Flynn, *Phys. Rev. Lett.* **57** 599 (1986).
- <sup>29</sup>S. C. Moss and D. L. Price, in *Physics of Disordered Materials*, edited by D. Adler, H. Fritzsche, and S. R. Ovshinsky (Plenum Press, New York, 1985), p. 77.
- <sup>30</sup>M. C. Wittels, *Philos. Mag.* **2**, 1445 (1957).
- <sup>31</sup>A. Bourret, J. Thibault-Desseaux, and D. N. Seidman, *J. Appl. Phys.* **55**, 825 (1984).
- <sup>32</sup>M. Castro-Colin, W. Donner, S. C. Moss, Z. Islam, S. K. Sinha, R. Nemanich, H. T. Metzger, P. Bösecke, and T. Shulli, preceding paper, *Phys. Rev. B* **71**, 045310 (2004).